Sodium and Chloride Concentrations, pH, and Depth of Airway Surface Liquid in Distal Airways

Yuanlin Song, Jay Thiagarajah, and A.S. Verkman

Departments of Medicine and Physiology, Cardiovascular Research Institute, University of California, San Francisco, CA, 94143

ABSTRACT The composition and depth of the airway surface liquid (ASL) are key parameters in airway physiology that are thought to be important in the pathophysiology of cystic fibrosis and other diseases of the airways. We reported novel fluorescent indicator and microscopy methods to measure [Na^+], [Cl^-], pH, and depth of the ASL in large airways (Jayaraman, S., Y. Song, L. Vetrivel, L. Shankar, and A.S. Verkman. 2001. *J. Clin. Invest.* 107:317–324.). Here we report a stripped-lung preparation to measure ASL composition and depth in small distal airways. Distal ASL was stained with ion- or pH-sensitive fluorescent indicators by infusion into mouse trachea of a perfluorocarbon suspension of the indicator. After stripping the pleura and limited microdissection of the lung parenchyma, airways were exposed for measurement of ASL [Na^+], [Cl^-], and pH by ratio imaging microscopy, and depth by confocal microscopy. The stripped-lung preparation was validated in stability and tissue viability studies. ASL [Na^+] was 122 ± 2 mM, [Cl^-] was 123 ± 4 mM and pH was 7.28 ± 0.07, and not dependent on airway size (<100- to >250-μm diameter), ENaC inhibition by amiloride, or CFTR inhibition by the thiazolidinone $CFTR_{inh}$-172. ASL depth was 8–35 μm depending on airway size, substantially less than that in mouse trachea of ~55 μm, and not altered significantly by amiloride. These results establish a novel lung preparation and fluorescence approach to study distal airway physiology and provide the first data on the composition and depth of distal ASL.

KEY WORDS: ASL • bronchioles • ratio imaging • lung • fluorescence microscopy

INTRODUCTION

The air-bathed surfaces of large and small airways are coated by a thin layer of fluid, the airway surface liquid (ASL), forming the interface between the luminal membrane of airway epithelial cells and the inspired/expired gas phase. The volume, ionic composition, and pH of the ASL are key physiological parameters that are related to airway hydration, reactivity, and antimicrobial activity. The determinants of ASL volume and composition probably include the rate of evaporative water loss, the transporting properties of the airway epithelium, the composition of fluid secreted onto the airway surface by submucosal glands, and the convective transport of fluid from lower to upper airways. It has been proposed that ASL volume and composition are important factors in the pathophysiology of cystic fibrosis, asthma, and other diseases of the airways (Smith et al., 1996; Boucher, 1999; Pilewski and Frizzell, 1999; Verkman et al., 2003).

The depth and composition of ASL in bronchial cell cultures and trachea have been studied by a variety of approaches, including microcapillary and filter paper sampling, rapid-freeze sampling, x-ray probe microanalysis, $^{22}Na^+$ and $^{36}Cl^-$ dilution, scanning confocal microscopy, and solid-state microelectrodes (for review see Boucher, 1999; Verkman et al., 2003). A wide range of ASL depths (<10 to >75 μm) has been estimated in tracheas of sheep, mouse, and guinea pig (Seybold et al., 1990; Rahmoune and Shephard, 1995; Jayaraman et al., 2001b). Also, a wide range of ASL [Na^+] and [Cl^-] has been reported (5–150 mM), in part because of technical difficulties in the measurement approaches such as the sampling of intracellular and interstitial fluids by microcapillary and filter paper methods. We recently introduced fluorescence methods to measure ASL [Na^+], [Cl^-], pH, osmolality, and depth in ASL of bronchial cell cultures, mouse trachea in vivo, and freshly obtained human bronchi. The ASL was stained with fluorescent dyes dispersed by sonication in volatile perfluorocarbon. Ratioable, membrane-impermeant fluorescent indicators were developed for measurement of ASL [Na^+] and [Cl^-] (Jayaraman et al., 2001b), and osmolality-sensitive liposomes were engineered for measurement of ASL osmolality (Jayaraman et al., 2001a). The ratioable pH indicator BCECF-dextran was used for ASL pH measurements (Jayaraman et al., 2001c), and ASL depth was determined by z-scanning confocal microscopy. In large airways ASL [Na^+] and [Cl^-] were 100–110 mM, pH 6.9–7.0, osmolality 300–325 mOsm, and depth 50–75 μm.

Address correspondence to Alan S. Verkman, 1246 Health Sciences East Tower, Cardiovascular Research Institute, University of California, San Francisco, San Francisco, CA 94143-0521. Fax: (415) 665-3847; email: verkman@itsa.ucsf.edu

Abbreviation used in this paper: ASL, airway surface liquid.

The purpose of this study was to measure the depth, ionic composition and pH in the ASL of distal airways, and to determine the role of key transporters that have been proposed to regulate ASL properties, including CFTR Cl^- channels and ENaC Na^+ channels. The challenges in these measurements are the inaccessibility of distal airways for fluid sampling and conventional optical measurements, and the inadequacy of cell-culture models and isolated airways for study of distal ASL properties. We developed a rapid procedure to stain the ASL with fluorescent indicators and to expose distal airways for observation by epifluorescence microscopy. ASL staining was accomplished by instillation into large airways of a perfluorocarbon suspension of the fluorescent dye, and small airways were exposed by pleural stripping and limited microdissection without direct trauma to the small airways being studied. The experiments here also utilize a long-wavelength ratioable Cl^- indicator that was developed recently for measurements of endosome $[Cl^-]$ (Sonawane et al., 2002), and a high-affinity thiazolidinone CFTR inhibitor identified recently by high-throughput screening (Ma et al., 2002). The methodology was validated and applied to measure the key ASL parameters in distal airways of mouse lung.

MATERIALS AND METHODS

Fluorescent Indicators

$[Na^+]$ was measured using a ratioable Na^+-sensitive fluorescent indicator prepared by incubation of carboxyl-modified latex beads (200-nm diameter) with the Na^+-sensitive, red fluorescent chromophore Corona Red™ (Molecular Probes) and the Na^+-insensitive, green fluorescent chromophore BODIPY-fl (Jayaraman et al., 2001b). Bead red-to-green fluorescence ratio (R/G) increased linearly with $[Na^+]$ from 0 to >200 mM and was not affected by pH. $[Cl^-]$ was measured using the ratioable Cl^- sensitive fluorescent indicator BAC-TMR-dextran synthesized as described previously (Sonawane et al., 2002), in which the Cl^--sensitive, green fluorescent chromophore BAC (10,10′-bis[3-carboxypropyl]-9,9′-biacridinium) was conjugated covalently to dextran (40 kD) together with the Cl^--insensitive, red fluorescent chromophore TMR (tetramethylrhodamine). BAC fluorescence is quenched by Cl^- by a collisional mechanism. Indicator red-to-green fluorescence ratio (R/G) increased linearly with $[Cl^-]$ from 0 to >200 mM Cl^- (Stern-Volmer constant 36 M^{-1}) and was not affected by pH. ASL pH was measured using the dual-excitation wavelength pH indicator BCECF (2′,7′-bis-[carboxyethyl]-5-carboxyfluorescein) conjugated to dextran (Molecular Probes). BCECF-dextran fluorescence measured at 490 and 440 nm excitation wavelengths (F_{490}/F_{440}) is pH sensitive with pKa ~7.0. Solution calibration of R/G versus $[Cl^-]$ (for BAC-TMR-dextran) and $[Na^+]$ (for Corona Red-BODIPY-bead) was done using PBS and Cl^-/NO_3^- and Na^+/choline$^+$ substitutions, respectively. Calibrations of F_{490}/F_{440} versus pH (for BCECF-dextran) were done using PBS titrated to specified pH with HCl/NaOH.

Stripped-lung Preparation and ASL Staining

Lungs were harvested from CD1 mice (age 6–8 wk). Mice were anesthetized with ketamine (40 mg/kg) and xylazine (8 mg/kg) intraperitoneally. The trachea was exposed by a midline incision and cannulated with PE-90 tubing. The abdominal aorta was transected and the heart and lung block was removed from the thoracic cavity for ASL staining and airway exposure as described below. To stain the ASL, 0.5 ml of volatile perfluorocarbon containing the dispersed ion or pH indicators (suspended by probe sonication) was infused into trachea to inflate the lungs, and excess fluid was removed by gentle suction. The visceral pleural membrane was stripped away from the lung parenchyma using forceps, starting from the hilum. Limited microdissection (generally taking <1 min) was then done using microdissection forceps under a stereo dissection microscope to expose some distal airways. The stripped-lung was then placed in a shallow 37°C Petri dish containing a premade agarose gel at the bottom (1% agarose in PBS). The Petri dish was transferred to a 37°C microincubator with flowing humidified 5% CO_2/95% O_2. A thin glass coverslip was positioned over the lung (without direct contact) for observation by epifluorescence microscopy. Condensation was prevented by blowing warmed air on the external surface of the coverslip.

Fluorescence Microscopy

Ratio imaging was done using a Nikon SMZ1500 stereo epifluorescence microscope equipped with 1.6× objective lens (numerical aperture 0.21, working distance 24 mm), cooled CCD camera (Photometrics), and custom filter sets (Chroma) for BAC, tetramethylrhodamine, Corona Red™, BODIPY-fl, and BCECF. ASL depth was measured using a Nipkow wheel-type confocal microscope (Leitz, with Technical Instruments confocal/coaxial module) equipped with a Nikon 50× extra-long working distance air objective (numerical aperture 0.55, working distance 8.5 mm). For ratio image analysis, images (2,000-ms acquisitions) were obtained from pairs of filter sets that were manually switched within <1 s. Photobleaching was insignificant for the Na^+ and pH indicators, and 3–5% per acquisition of a BAC image for the Cl^- indicator. BAC photobleaching was minimized by identifying distal airways with the TMR filter set and illuminating the lung at the BAC excitation wavelength only during image acquisition.

Measurements of Ionic Composition and pH

ASL $[Na^+]$ was measured from red (Corona Red™) and green (BODIPY-fl) images taken of airways stained with fluorescent Na^+-sensing beads. ASL $[Cl^-]$ was measured from red (TMR) and green (BAC) images of BAC-TMR-dextran–stained airways, and ASL pH was measured from green (BCECF) images taken at 490 and 440 nm excitation wavelengths. Fluorescence ratios were computed (pixel-by-pixel or over regions of interest) after subtraction of background determined from the average of four regions outside of the fluorescent airway. $[Na^+]$, $[Cl^-]$, or pH were determined from fluorescence ratios using calibrations as described above. In some experiments, a transport inhibitor (amiloride 10 mg/kg, $CFTR_{inh}$-172 1.2 mg/kg) was injected intraperitoneally 45–60 min before experiments. Dosages of amiloride and $CFTR_{inh}$-172 were chosen from previous in vivo mouse studies (Lee and Tannock, 1996; Ma et al., 2002). In some experiments mouse lungs were perfused with Na^+-free (replaced by choline$^+$) or Cl^--free (replaced by NO_3^-) solutions for 45 min at a pressure of 8 cmH_2O before experiments, or the perfusate contained hyperosmolar saline (PBS containing 300 mM mannitol).

Measurements of Distal ASL Depth

ASL depth was measured by confocal imaging of the airways after staining with the brightly red-fluorescing TMR-dextran. The axial and in-plane resolutions (point-spread-functions) of the optical system for intralumenal airway measurements were quanti-

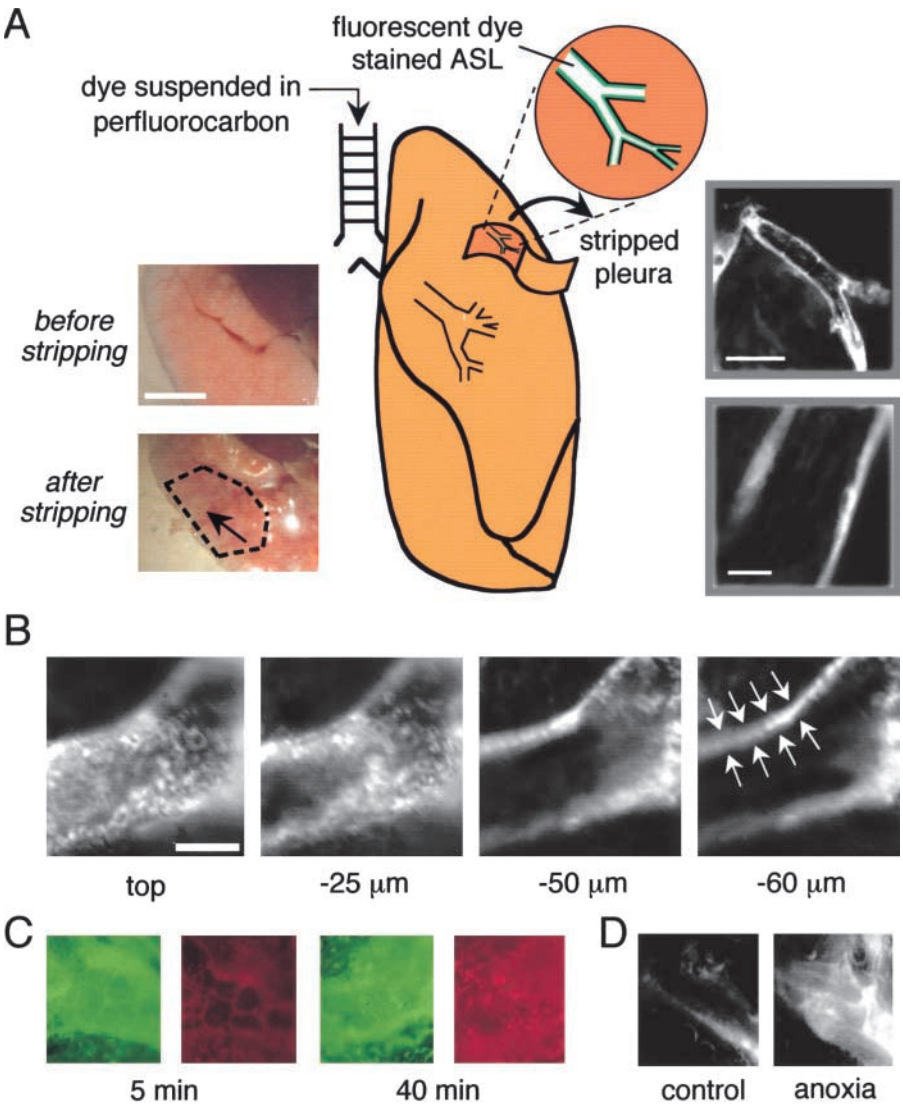

FIGURE 1. Stripped-lung preparation for visualization of fluorescently stained distal airway surface liquid. (A) Schematic of method for ASL staining and exposure of small airways. As described in MATERIALS AND METHODS, fluorescent dye in a perfluorocarbon suspension was instilled into the trachea, and small airways were exposed by pleural stripping and limited parenchymal microdissection. (Left inset) Brightfield low magnification images of airway preparation before and after (region bounded by black dashes) pleural stripping. Black arrow points to a visible airway. Bar, 5 mm. (Right inset) Low and high magnification wide-field fluorescence micrographs after ASL staining with TMR-dextran. Bars: 500 μm (top) and 100 μm (bottom). (B) Confocal fluorescence images taken at indicated depths into a distal airway. White arrows point to fluorescently-stained ASL. Bar, 50 μm. (C) Viability of airway epithelia studied using a live/dead stain (green for live cells and red for dead cells). Fluorescence micrographs taken at 5 min (left) and 40 min (right). (D) Images as in B, taken after distal ASL staining with the small polar dye sulforhodamine 101 before (left) and at 10 min after anoxia (right).

fied by imaging red-fluorescent latex beads (Molecular Probes) of diameters 3.7 and 9.7 μm introduced into the distal ASL. ASL depths were computed by deconvolution, as described previously (Jayaraman et al., 2001b), of fluorescence profiles perpendicular to the airway wall of sharply focused airways. To validate the confocal system for determination of the thickness of annular fluorescent layers, airway-size glass micropipettes were imaged in various configurations as described in RESULTS.

Alveolar Fluid Clearance

Using established methods, mice were anesthetized with ketamine (40 mg/kg) and xylazine (8 mg/kg), the trachea cannulated with PE90 tubing, and the abdominal aorta transected. Body temperature was maintained at 37°C using a heating pad and heat lamp. 0.25 ml PBS containing 5% bovine albumin and ^{131}I-albumin (1 μCi/ml) was infused into the lung (pH 7.4, 320 mOsm), and the tracheal cannula was connected to 100% O_2 at constant 5-cm H_2O pressure. In some experiments the instillate contained 100 μM isoproterenol. At 30 min, 0.1–0.2 ml fluid was collected via the cannula for measurement of ^{131}I-albumin radioactivity. In some experiments amiloride was infused intraperitoneally before clearance measurements.

RESULTS

As diagrammed in Fig. 1 A, the ASL throughout large and small airways was stained with fluorescent indicators by infusion of a perfluorocarbon suspension of the indicator into the mouse trachea. As found previously in cell cultures grown at an air–liquid interface and intact trachea (Jayaraman et al., 2001b), the suspended indicator dissolved rapidly in the aqueous ASL and became fluorescent. For visualization by epifluorescence microscopy, distal airways were exposed by pleural stripping and limited microdissection of the superficial lung parenchyma (Fig. 1 A). The photographs on the left show a mouse lung before and after stripping. Airways can be seen (black arrow) within the stripped region (bounded by black dashes). The wide-field fluorescence micrographs at the right show stained ASL in airways (at low and high magnification) just after perfluorocarbon infusion and pleural stripping/microdissection. Airways with this typical staining pattern were

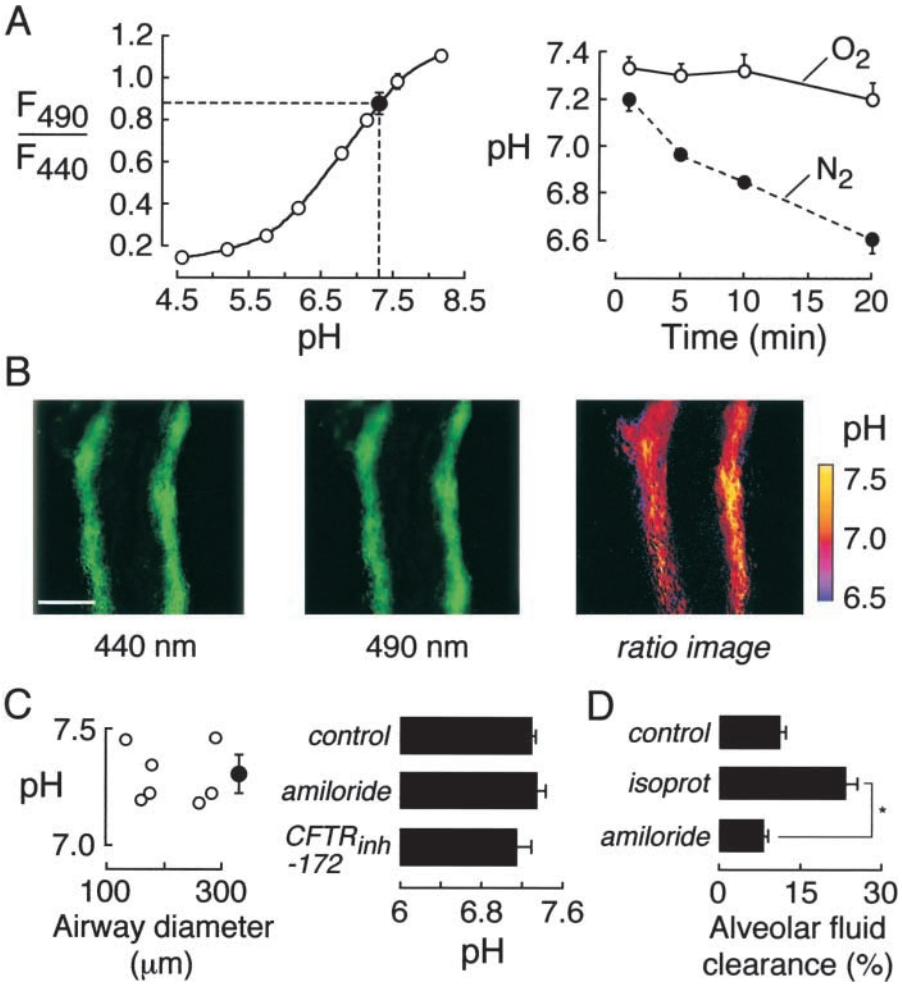

FIGURE 2. ASL pH in mouse distal airways. The ASL was stained with BCECF-dextran. (A, left) Ratio of BCECF-dextran green fluorescence measured at 490- and 440-nm excitation wavelengths (F_{490}/F_{440}) as a function of pH in in vitro measurements (open circles). Also shown is averaged F_{490}/F_{440} and deduced pH in ASL of distal airways (filled circle). (Right) Time course of ASL pH in distal airways exposed to O_2 (humidified, with 5% CO_2) versus N_2 at 37°C. (B) Fluorescence images of BCECF-dextran-stained distal airway taken at 440 nm (left) and 490 nm (middle) excitation wavelengths. Spatial map of ASL pH shown as pseudocolored ratio image (right). Bar, 100 μm. (C) ASL pH measured in airways of indicated size (left) and after administration of inhibitors (right) (mean ± SE, n = 8–12 airways). (D) Alveolar fluid clearance (percentage absorption at 30 min) in lungs at 37°C after tracheal fluid instillation of PBS ("control") or isoproterenol ("isoprot", 100 μM). Where indicated ("amiloride"), mice were given amiloride (10 mg/kg i.p.) 45 min before measurement (isoproterenol present in the instillate). *$P < 0.001$.

used for analysis of ASL $[Na^+]$, $[Cl^-]$, pH, and depth. Fig. 1 B shows four images out of a series taken at increasing depths through a distal airway. The image on the right was taken approximately through the center of the airway, showing most of the stained ASL in focus.

Control studies were done to verify the viability of the mouse lung preparation used for distal ASL studies. Airway cells were stained after instillation of a live/dead vital stain in which live cells appear green and dead cells red. Less than 1% dead cells were seen for at least 5–10 min under the conditions of the experiments (37°C, 5% CO_2 humidified atmosphere) (Fig. 1 C, left). Dead cells were readily visible after 40 min (Fig. 1 C, right) or 10 min of anoxia (unpublished data). In other measurements (see below) distal ASL ionic composition and pH remained stable for at least 10 min under the conditions of the experiments. Ciliary beating in larger airways was observed for 45–60 min in the preparation, but ceased within a few minutes after anoxia. To assess paracellular permeability, the distal ASL was stained with the small polar (red-fluorescing) fluorophore sulforhodamine 101. This small probe remained confined to the ASL under the experimental conditions as shown by fluorescence confocal microscopy (Fig. 1 D, left), but leaked out of vessels after 10 min of anoxia (Fig. 1 D, right). Finally, a function of distal airway epithelial cells, cytoplasmic pH regulation, as assessed by ratio imaging after in situ cell loading with BCECF-AM introduced into the airways. Cytoplasmic pH was stable at 7.24–7.32 under the experimental conditions, but promptly acidified (<6.8) after 10 min of anoxia. All measurements of distal ASL composition and depth were done within 10 min after pleural stripping/microdissection and warming to 37°C.

The ionic content and pH of distal ASL was determined by ratio image analysis using ratioable fluorescent indicators. ASL pH was measured using the pH indicator BCECF-dextran, where the ratio of green fluorescence when excited at 490 and 440 nm (F_{490}/F_{440}) is strongly pH-dependent with pKa ~7.0. Fig. 2 A (left) shows a solution calibration of BCECF-dextran together with average distal ASL pH. All measurements were done under physiological conditions in the presence of a 37°C humidified atmosphere containing 5% CO_2. Fig. 2 A (right) shows that distal ASL pH re-

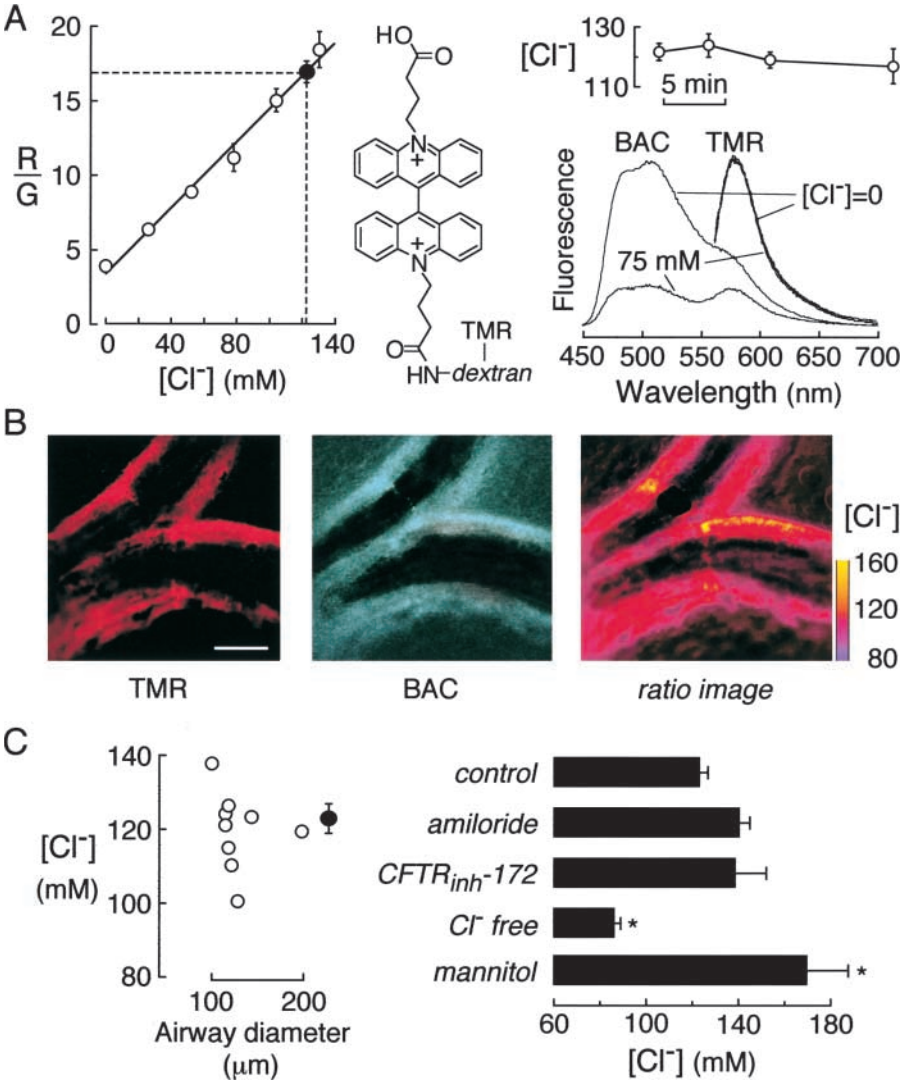

FIGURE 3. [Cl⁻] in ASL of mouse distal airways. The ASL was stained with BAC-TMR-dextran, containing green-fluorescing Cl⁻-sensitive BAC and red-fluorescing Cl⁻-insensitive TMR chromophores. (A, left) Ratio of red-to-green fluorescence (R/G) of as a function of [Cl⁻] in vitro. Measurements done in PBS in which Cl⁻ was replaced by NO_3^- (open circles). Also shown in averaged R/G and deduced [Cl⁻] in ASL of distal airways (filled circle). (Middle) Chemical structure of BAC-TMR-dextran. (Right, top) Time course of ASL [Cl⁻] in distal airways. (Right, bottom) Fluorescence emission spectra of BAC-TMR-dextran in PBS containing 0 or 75 mM Cl⁻ (NO_3^- replacing Cl⁻). (B) Red (left) and green (middle) images of BAC-TMR-dextran–stained distal airways. Spatial map of ASL [Cl⁻] shown as pseudocolored ratio image (right). Bar, 100 μm. (C) ASL [Cl⁻] measured in airways of indicated size (left) and after indicated maneuvers (right). Maneuvers include ENaC and CFTR inhibition, pulmonary artery perfusion with 0 Cl⁻ buffer for 45 min before measurements ("Cl⁻ free"), and hypertonic solution ("mannitol") where perfusion was done for 45 min with PBS + 300 mM mannitol.

mained stable for at least 10 min under the experimental conditions. However, ASL pH decreased promptly after inducing tissue hypoxia by replacing atmospheric oxygen by nitrogen. Fig. 2 B shows representative wide-field fluorescence images of the BCECF green fluorescence excited at 440 nm (left) and 490 nm (middle), together with a pseudocolored ratio image map of ASL pH (right). Distal ASL pH was quite uniform with standard deviation generally <0.1 (when averaged in 5-μm bins). Fig. 2 C summarizes ASL pH in airways of different sizes (left) and in distal airways after inhibitors (right). Averaged ASL pH was 7.28 and not dependent on airway diameter. Distal ASL pH was not changed significantly after ENaC or CFTR inhibition by amiloride and $CFTR_{inh}$-172, respectively.

The concentrations of amiloride and $CFTR_{inh}$-172 for intraperitoneal administration (45 min before experiments) were high to ensure adequate block at the time of the experiments. To verify the amiloride block, alveolar fluid clearance was measured in lungs at 30 min after administration of amiloride as done on the distal ASL studies. In control (no amiloride) lungs, alveolar fluid clearance was 12% in 30 min under basal conditions and 22% when isoproterenol was included in the tracheal instillate. In lungs from amiloride-treated mice, alveolar fluid clearance (measured with isoproterenol) was reduced to 7% ($P < 0.001$), indicating adequacy of ENaC block. For $CFTR_{inh}$-172, we have reported that intraperitoneal infusion of 20 μg (50% of dose given here) blocked cholera toxin–induced intestinal fluid secretion by >90% (Ma et al., 2002). Further analysis showed $CFTR_{inh}$-172 efficacy over 6–9 h in mice and 50% block of fluid secretion after a single 5-μg intraperitoneal dose (Thiagarajah et al., 2003).

For measurement of ASL [Cl⁻], the indicator consisted of a 40,000-dalton dextran conjugated to a green-fluorescing Cl⁻-sensitive fluorophore (BAC) and a red-fluorescing Cl⁻-insensitive fluorophore (TMR) (Fig. 3 A, middle), such that the red-to-green fluorescence ratio (R/G) provided a quantitative measure of [Cl⁻].

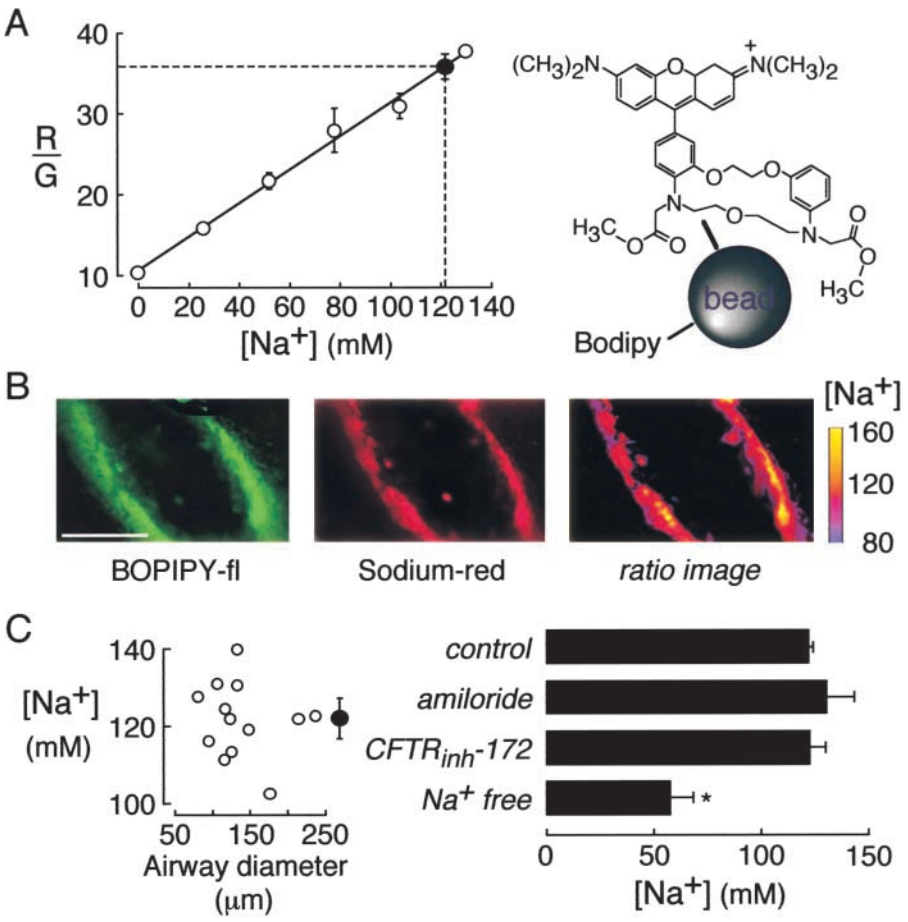

FIGURE 4. [Na^+] in ASL of mouse distal airways. The ASL was stained with 200-nm diameter polystyrene beads containing Na^+-sensitive Corona red™ (red fluorescing) and Na^+-insensitive BODIPY-fl (green fluorescing). (A) Ratio of red-to-green fluorescence (R/G) of the Na^+ indicator as a function of [Na^+] in PBS in which Na^+ was replaced by choline$^+$ (open circles). Also shown in averaged R/G and deduced [Na^+] in ASL of distal airways (filled circle). (B) Green (left) and red (middle) images of fluorescently-stained distal airways. Spatial map of ASL [Na^+] shown as pseudocolored ratio image (right). Bar, 100 μm. (C). ASL [Na^+] measured in airways of indicated size (left) and after indicated maneuvers (right). Maneuvers include ENaC and CFTR inhibition, and pulmonary artery perfusion with 0 Na^+ buffer for 45 min before measurements ("Na^+ free").

Fig. 3 A (left) shows a solution calibration of R/G versus [Cl^-] in which the indicator was suspended in phosphate buffer saline with NO_3^- replacing Cl^-. Also shown is average R/G measured in ASL of distal airways. Fig. 3 A (right, top) shows that ASL [Cl^-] was stable for at least 15 min in repeated measurements. Fig. 3 A (right, bottom) gives fluorescence spectra of the ratioable fluorescent dextran, showing decreased BAC but not TMR fluorescence at 75 versus 0 mM Cl^-. Fig. 3 B shows representative wide-field fluorescence images of the red (left) and green (middle) channels, together with a pseudocolored ratio image map of ASL [Cl^-] (right). Fig. 3 C summarizes ASL [Cl^-] in airways of different sizes (left) and in distal airways after inhibitors and pulmonary artery perfusion with Cl^- free or hypertonic buffers (right). Averaged ASL [Cl^-] was 123 mM and not dependent on airway diameter. As expected, distal ASL [Cl^-] decreased after pulmonary artery perfusion with Cl^- free solution, and increased after perfusion with hyperosmolar (600 mOsm) solution to dehydrate the ASL. Distal ASL [Cl^-] was not sensitive to ENaC or CFTR inhibition.

For measurement of ASL [Na^+], the indicator was a small polystyrene bead containing a red-fluorescing Na^+-sensitive fluorophore (Corona Red™) and a green-fluorescing Na^+-insensitive fluorophore (BODIPY-fl) such that the red-to-green fluorescence ratio (R/G) provided a quantitative measure of [Na^+] (Fig. 4 A, right). Fig. 4 A (left) shows a solution calibration of R/G versus [Na^+] in which beads were suspended in PBS with choline$^+$ replacing Na^+. Also shown is average R/G measured in ASL of distal airways. Fig. 4 B shows representative wide-field fluorescence images of the red (left) and green (middle) channels, together with a pseudocolored ratio image map of ASL [Na^+] (right). Fig. 4 C summarizes ASL [Na^+] in airways of different sizes (left) and in distal airways after indicated maneuvers (right). Averaged ASL [Na^+] was 122 mM and not dependent on airway diameter. As expected, ASL [Na^+] decreased after perfusion of the pulmonary artery with Na^+ free solution for 45 min. Distal ASL [Na^+] was not sensitive to ENaC or CFTR inhibition.

The depth (thickness) of the distal ASL was estimated by confocal fluorescence microscopy after staining with the bright red fluorescent indicator TMR-dextran. Fig. 5 A, a–d, shows a gallery of high-magnification confocal micrographs of small airways of different diameters. The stained ASL in each case is seen as a distinct band of fluorescence. Fig. 5 B shows profiles of fluorescence through regions of the ASL as demarcated by the dashed white lines in A, along with fitted Gaussian functions. To determine ASL depth from the

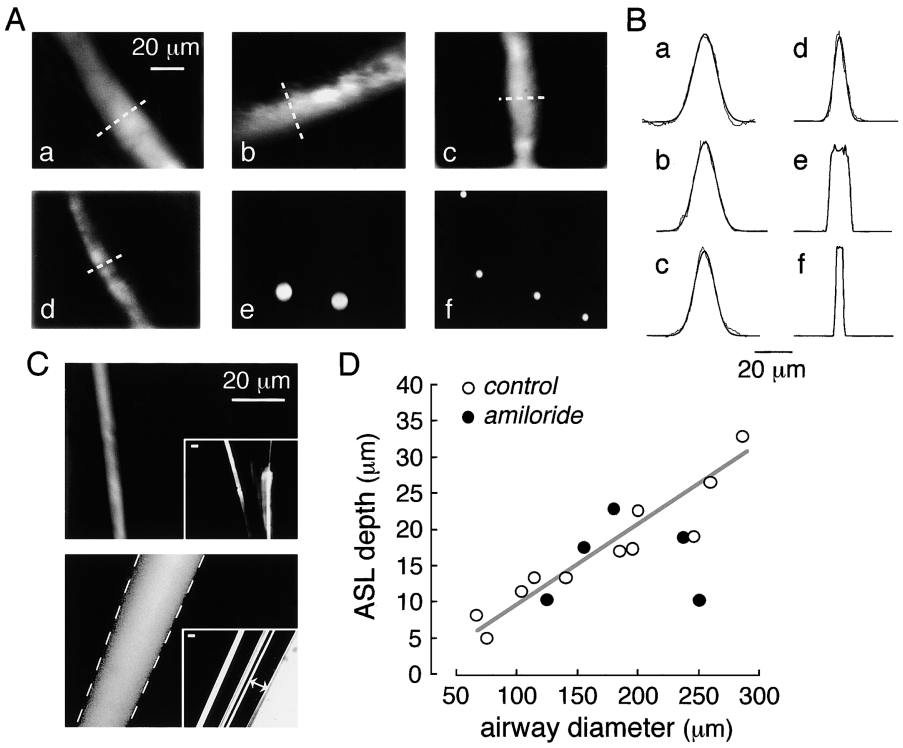

FIGURE 5. ASL depth in mouse distal airways. (A) Representative fluorescence confocal images of TMR-dextran–stained ASL in distal airways of different diameters. Stained ASL (only one edge of airway) shown at high magnification. Airway diameters were 260, 200, 185, and 105 μm for a–d, respectively. Confocal images of red fluorescent latex beads of 9.7 and 3.7 μm diameter shown in e and f. (B) Fluorescence scans taken at indicated regions of ASL from images in a–d in A (dashed lines) along with fitted Gaussian functions (smooth curves). Scans taken through center of beads for e and f. (C, top) Fluorescence confocal image of glass micropipette coated with a submicron fluorescent layer (by dipping in chloroform containing dissolved green-fluorescing polystyrene beads). Inset shows low magnification wide-field fluorescence. (Bottom) Fluorescence confocal image taken at the center of concentric glass micropipettes sandwiching an annular fluorescent aqueous layer (TMR-dextran in water). Dashed lines show boundary of inner and outer micropipettes determined from brightfield micrographs as shown in the inset (lines with double arrows). Bars, 20 μm. (D) ASL depth as a function of airway diameter determined by reconvolution of scans as in B (open circles, control mice; closed circles, amiloride-treated mice). Differences in control versus amiloride-treated mice not significant.

fluorescence profiles, the resolution of the optical system was characterized by imaging of red fluorescent beads (3.7- and 9.7-μm diameters) introduced into the ASL as suspensions in perfluorocarbon. Fig. 5 A, e and f, shows bead images, with the corresponding fluorescence profiles shown in Fig. 5 B. As a further test of the optical system, confocal images of fluorescent micropipettes were obtained for an annular fluorescent layer as in distal airways. Fig. 5 C (top) shows a confocal fluorescence image of a micropipette in which a submicron fluorescent layer was deposited onto the pipette surface (inset: low magnification image). The apparent thickness of the fluorescent layer was 3–4 μm. Fig. 5 C (bottom) shows an image of an annular fluorescent aqueous fluid layer trapped between concentric micropipettes. The apparent thickness of the fluid layer agreed well with the actual thickness (dashed white lines) determined from brightfield images as seen in the inset. From these studies we conclude that distal ASL depths down to 4 μm can be measured.

Distal ASL depths are summarized in Fig. 5 D. ASL depth increased with greater airway diameter. Measurements of distal ASL depth were also performed in five mice (closed circles) after amiloride treatment under conditions shown above to effectively block alveolar fluid clearance. Distal ASL depth did not differ significantly in amiloride- versus nonamiloride-treated mice.

DISCUSSION

Novel methodology was developed for fluorescence measurement of ionic composition, pH, and depth of ASL in intact distal airways. Introduction of engineered ratioable fluorescent indicators into the ASL using a volatile perfluorocarbon suspension permitted rapid ASL staining without perturbing ASL volume and composition with aqueous dye solutions. Distal airways with fluorescently stained ASL were visualized by stripping the visceral pleural membrane and dissecting a small amount of tissue near the lung surface. Fluorescent dyes that remained confined to the ASL compartment were used for in situ measurements of ASL [Na^+], [Cl^-], and pH by ratio imaging fluorescence microscopy, and ASL depth by confocal microscopy.

The lung preparation for examination of the distal ASL involved lung removal from mice, introduction of a perfluorocarbon suspension of dye into the airways, pleural stripping, and limited parenchymal microdissection. The preparation was generally completed <5 min after lung removal. Several different assessments suggested the viability of the preparation, including vital dye exclusion, constancy of ASL properties, maintenance of paracellular integrity, ciliary beating, and airway cell pH regulation. Appropriate controls showed that these parameters were sensitive to hypoxic tissue injury. However, since the measurement process did re-

quire lung manipulation and dye solution instillation, we cannot be certain that some airway properties and epithelial cell transporters were perturbed.

The technical details and validation of the dyes and microscopy methods were established in prior measurements of ASL properties in cell-culture models and large airways (Jayaraman et al., 2001b). However, the ratioable quinolinium-based Cl^- indicator used previously was not suitable for measurement of distal ASL [Cl^-] because of high background fluorescence of the lung preparation at the 450-nm emission wavelength of the quinolinium chromophore. The long-wavelength ratioable Cl^- indicator BAC-TMR-dextran used here was developed recently for measurement of the kinetics and regulation of endosomal [Cl^-] in cell culture models (Sonawane et al., 2002). The BAC acridinium chromophore is green fluorescent, Cl^- selective, and pH insensitive under the conditions of the experiments. Quantitative ratio imaging permitted determination of distal ASL [Na^+] and [Cl^-] to better than ~3 mM accuracy and pH to better than ~0.05 unit accuracy. Distal ASL depth was estimated by confocal microscopy of airways after staining with a brightly red-fluorescing dye. Confocal imaging of red fluorescent beads introduced into the airways, and of fluorescent glass micropipettes verified spatial resolution of better than 4 μm.

Limited information is available about the transport properties of the distal airway epithelium. By immunostaining and immunoblot analysis, distal airway epithelial cells express ENaC Na^+ channels, CFTR Cl^- channels, AQP4 water channels, and ClC-type Cl^- channels (Frigeri et al., 1995; Nielsen et al., 1997; Rochelle et al., 2000; Song et al., 2001; Edmonds et al., 2002). Few perfusion studies of distal airways have been reported due in part to difficulties in microdissection and microperfusion. Our lab measured osmotically driven water transport in microperfused guinea pig distal airways using a lumenal fluorescent indicator to deduce water flow across the epithelial barrier (Folkesson et al., 1996). Osmotic water permeability was moderately high, weakly temperature-sensitive, and not inhibited by mercurials, consistent with the expression of AQP4 on the basolateral membrane of distal airway epithelial cells. In microperfused human distal airways, Blouquit et al. (2002) reported that the transmural potential difference was increased by cAMP agonists and inhibited by luminal amiloride. Na^+ and Cl^- absorption were demonstrated in microperfused distal airways from sheep (Al-Bazzaz, 1994). Studies in Clara cell cultures showed net fluid absorption driven by Na^+ transport (Van Scott et al., 1989). A recent study on primary cultures of human distal airway epithelial cells reported increased short-circuit current in response to foskolin and ATP (Blouquit et al., 2002), which was inhibited by amiloride. Also, indirect evidence showing inhibition of cAMP-stimulated airway fluid absorption and Cl^- transport by CFTR inhibitors (Fang et al., 2002) suggested that the distal airways can carry out isosmolar fluid absorption as do large airways (Song et al., 2001) and alveoli (Matthay et al., 2000). Thus, the distal airway epithelium appears to be capable of significant ion and water transport; however, the limited information about transporting mechanisms precluded analysis of ASL properties of distal airways in terms of epithelial transporting mechanisms.

The depth of the ASL was 55 μm in mouse trachea (Jayaraman et al., 2001c), decreasing to ~10 μm in distal airways. A small ASL depth in mouse distal airways of <75-μm diameter permits relatively unobstructed air flow which could not occur if the distal airways were lined by a 55-μm thick ASL as in trachea. The greater ASL depth in more proximal airways may result from upward fluid convection, differences in the surface properties of airway epithelial cells, and/or axial heterogeneity in ion transport properties. Our data agree with the results of Widdicombe et al. (1997) that ASL depth gradually decreased after bifurcation of airways, which they proposed was due to differential absorption of airway fluid.

The mechanisms responsible for regulation of ASL depth remain uncertain. One theory suggests the ASL depth is regulated by sensors in the epithelial cell regulating ion transport (Tarran et al., 2002), but so far no sensors have been identified. It is believed that CFTR deletion is associated with increased ENaC activity, and there is evidence in airway cell-culture models that ASL depth is reduced in cells derived from cystic fibrosis human airways (Matsui et al., 1998). However, reduced ASL depth was not found in ΔF508 mice (Jayaraman et al., 2001b) and appropriate studies have not been done in human airways. We found here that ENaC inhibition by amiloride did not affect distal ASL depth in the steady-state, suggesting that ENaC does not play a role in regulating steady-state distal ASL depth. However, we cannot rule out the possibility that ENaC function was impaired in our preparation, or that a role for ENaC in regulating distal ASL depth might be seen under stressed conditions not tested here.

The ionic composition and pH of ASL fluid did not depend on airway size. Sodium and chloride concentrations were in the range 120–125 mM and pH was 7.2–7.3. Because airways are water permeable (Folkesson et al., 1996; Matsui et al., 2000), rapid osmotic water movement should effectively clamp ASL osmolality to that of epithelial cell cytoplasm and serum, as was found for ASL osmolality in large airways (Jayaraman et al., 2001b). The remaining ASL constituents involved in osmotic balance, K^+, HCO_3^-, and small nonionic solutes (urea, glucose, and amino acids), are present in the ASL at substantially lower concentration than Na^+ and Cl^-. The constancy of ASL Na^+ and Cl^- concentrations may thus result from constraints imposed by osmotic (and ionic charge) balance. Based on our previ-

ous studies of mechanisms regulating ASL pH in bronchial cell cultures and mouse trachea (Jayaraman et al., 2001c), the constancy of ASL pH probably results from constraints imposed by the tightly regulated pH of serum and epithelial cell cytoplasm, which are in contact with the highly H^+/OH^--permeable epithelial barrier. However, these considerations remain speculative until a rigorous description is available of the mechanisms regulating ASL composition and volume.

In summary, we have developed a stripped-lung preparation and fluorescent dye/microscopy methods to measure ASL properties in situ in intact distal airways in mouse lung. The ability to visualize fluorescently stained ASL in mouse distal airways should make it possible to carry out similar studies in human lung. ASL depth in distal airways of mouse lung was substantially less than in larger central airways, but ionic composition and pH were similar. The insensitivity of the ionic composition and pH of the distal ASL to CFTR and/or ENaC inhibition suggests that these ion channels do not play a major role in regulating steady-state compositon of the distal ASL.

We thank Liman Qian for mouse breading and Dr. Michael Matthay for helpful suggestions, and Dr. Nitin Sonawane for synthesis of BAC-TMR-dextran.

This work was supported by grants HL73856, HL59198, DK35124, EB00415, and EY13574 from the National Institutes of Health, and Research Development Program grant R613 from the Cystic Fibrosis Foundation. Dr. Song was supported by a research training fellowship from American Lung Association of California, and Dr. Jay Thiajarajah by a fellowship from the Cystic Fibrosis Foundation.

Lawrence G. Palmer served as editor.

Submitted: 12 May 2003
Accepted: 11 September 2003

REFERENCES

Al-Bazzaz, F.J. 1994. Regulation of Na and Cl transport in sheep distal airways. *Am. J. Physiol.* 267:L193–L198.

Blouquit, S., H. Morel, J. Hinnrasky, E. Naline, E. Puchelle, and T. Chinet. 2002. Characterization of ion and fluid transport in human bronchioles. *Am. J. Respir. Cell Mol. Biol.* 27:503–510.

Boucher, R.C. 1999. Molecular insights into the physiology of the 'thin film' of airway surface liquid. *J. Physiol.* 516:631–638.

Edmonds, R.D., I.V. Silva, W.B. Guggino, R.B. Butler, P.L. Zeitlin, and C.J. Blaisdell. 2002. ClC-5: ontogeny of an alternative chloride channel in respiratory epithelia. *Am. J. Physiol.* 282:L501–L507.

Fang, X., N. Fukuda, P. Barbry, C. Sartori, A.S. Verkman, and M.A. Matthay. 2002. Novel role for CFTR in fluid absorption from the distal airspaces of the lung. *J. Gen. Physiol.* 119:199–207.

Folkesson, H.G., M.A. Matthay, A. Frigeri, and A.S. Verkman. 1996. High transepithelial water permeability in microperfused distal airways: evidence for channel-mediated water transport. *J. Clin. Invest.* 97:664–671.

Frigeri, A., M. Gropper, C.W. Turck, and A.S. Verkman. 1995. Immunolocalization of the mercurial-insensitive water channel and glycerol intrinsic protein in epithelial cell plasma membranes. *Proc. Natl. Acad. Sci. USA.* 92:4328–4331.

Jayaraman, S., Y. Song, and A.S. Verkman. 2001a. Airway surface liquid osmolality measured using fluorophore-encapsulted liposomes. *J. Gen. Physiol.* 117:423–430.

Jayaraman, S., Y. Song, L. Vetrivel, L. Shankar, and A.S. Verkman. 2001b. Non-invasive fluorescence measurement of salt concentration in the airway surface liquid. *J. Clin. Invest.* 107:317–324.

Jayaraman, S., Y. Song, and A.S. Verkman. 2001c. Airway surface liquid pH in well-differentiated airway epithelial cell cultures and mouse trachea. *Am. J. Physiol.* 281:C1504–C1511.

Lee, C., and I. Tannock. 1996. Pharmacokinetic studies of amiloride and its analogs using reversed-phase high-performance liquid chromatography. *J. Chromatogr. B Biomed. Appl.* 685:151–157.

Ma, T., J.R. Thiagarajah, H. Yang, N.D. Sonawane, C. Folli, L.J. Galietta, and A.S. Verkman. 2002. Thiazolidinone CFTR inhibitor identified by high-throughput screening blocks cholera toxin-induced intestinal fluid secretion. *J. Clin. Invest.* 110:1651–1658.

Matsui, H., B.R. Grubb, R. Tarran, S.H. Randell, J.T. Gatzy, C.W. Davis, R.C. Boucher. 1998. Evidence for periciliary liquid layer depletion, not abnormal ion composition, in the pathogenesis of cystic fibrosis airways disease. *Cell.* 95:1005–1015.

Matsui, H., C.W. Davis, R. Tarran, and R.C. Boucher. 2000. Osmotic water permeability of cultured, well-differentiated normal and cystic fibrosis airway epithelia. *J. Clin. Invest.* 105:1419–1427.

Matthay, M.A., N. Fukuda, J. Frank, R. Kallet, B. Daniel, and T. Sakuma. 2000. Alveolar epithelial barrier. Role in lung fluid balance in clinical lung injury. *Clin. Chest Med.* 21:477–490.

Nielsen, S., L.S. King, B.M. Christensen, and P. Agre. 1997. Aquaporins in complex tissues. II. Subcellular distribution in respiratory and glandular tissues of rat. *Am. J. Physiol.* 273:C1549–C1561.

Pilewski, J.M., and R.A. Frizzell. 1999. Role of CFTR in airway disease. *Physiol. Rev.* 79:S215–S255.

Rahmoune, H., and K.L. Shephard. 1995. State of airway surface liquid on guinea pig trachea. *J. Appl. Physiol.* 78:2020–2024.

Rochelle, L.G., D.C. Li, H. Ye, E. Lee, C.R. Talbot, and R.C. Boucher. 2000. Distribution of ion transport mRNAs throughout murine nose and lung. *Am. J. Physiol.* 279:L14–L24.

Seybold, Z.V., A.T. Mariassy, D. Stroh, C.S. Kim, H. Gazeroglu, and A. Wanner. 1990. Mucociliary interaction in vitro: effects of physiological and inflammatory stimuli. *J. Appl. Physiol.* 68:1421–1426.

Smith, J.J., S.M. Travis, E.P. Greenberg, and M.J. Welsh. 1996. Cystic fibrosis airway epithelia fail to kill bacteria because of abnormal airway surface fluid. *Cell.* 85:229–236.

Sonawane, N., J.R. Thiagarajah, and A.S. Verkman. 2002. Chloride concentration in endosomes measured using a ratioable fluorescent Cl^- indicator: evidence for Cl^- accumulation during acidification. *J. Biol. Chem.* 277:5506–5513.

Song, Y., S. Jayaraman, B. Yang, M.A. Matthay, and A.S. Verkman. 2001. Role of aquaporin water channels in airway fluid transport, humidification and surface liquid hydration. *J. Gen. Physiol.* 117:573–582.

Tarran, R., M.E. Loewen, A.M. Paradiso, J.C. Olsen, M.A. Gray, B.E. Argent, R.C. Boucher, and S.E. Gabriel. 2002. Regulation of murine airway surface liquid volume by CFTR and Ca^{++}-activated Cl^- conductances. *J. Gen. Physiol.* 120:407–418.

Thiagarajah, J., T. Broadbent, and A.S. Verkman. 2003. Prevention of toxin-induced intestinal ion and fluid secretion by a small-molecule CFTR inhibitor. *Gastroenterology.* In press.

Van Scott, M.R., C.W. Davis, and R.C. Boucher. 1989. Na^+ and Cl^- transport across rabbit nonciliated bronchiolar epithelial (Clara) cells. *Am. J. Physiol.* 256:C893–C901.

Verkman, A.S., Y. Song, and J.R. Thiagarajah. 2003. Role of airway surface liquid and submucosal glands in cystic fibrosis lung disease. *Am. J. Physiol.* 284:C2–C15.

Widdicombe, J.H., S.J. Bastacky, D.X. Wu, and C.Y. Lee. 1997. Regulation of depth and composition of airway surface liquid. *Eur. Respir. J.* 10:2982–2987.